Limitations of the shallow water assumptions for problems involving steep slopes: application to a dike overtopping test case

S. Van Emelen
Fond de la Recherche Scientifique – FNRS & Institute of Mechanics, Materials and Civil Engineering, Université catholique de Louvain, Louvain-la-Neuve, Belgium

Y. Zech & S. Soares-Frazão
Institute of Mechanics, Materials and Civil Engineering, Université catholique de Louvain, Louvain-la-Neuve, Belgium

ABSTRACT: This paper proposes an analysis of the limitations of the low-slope assumption in the shallow water models for problems involving rather steep slopes. First, the equations including the steep slope effect are presented in one dimension and compared to the classical shallow-water equations. Both models are solved with a first-order classical finite volume scheme, using a lateralised HLL solver for the fluxes computation. The models give comparable results when compared on fast transient flows on steep slopes, while they differ when modelling uniform steady flows. They also lead to comparable results in the particular case of a flow overtopping a dike. Finally, the impact of the classical shallow water assumptions on the sediment transport evaluation is analysed. Comparable conclusions are drawn for sediment transport modelling, showing that the classical shallow water model is suitable for fast transient flows, but more accurate models should be used when modelling erosion for steady uniform flows.

1 INTRODUCTION

Breaching of earthen dikes or levees involves complex processes, and the resulting breaches can lead to major floods and consequent damages. The understanding of these phenomena and their accurate modelling are important for flood prediction, risk assessment and rescue planning.

Numerical models based on classical Saint-Venant equations are generally used to simulate breaching processes because of their ease of use, and their ability to deal with complex topographies. They also allow for an easy insertion of sediment transport processes. However, these shallow-water models are based on quite restrictive assumptions that are not always fulfilled in real cases. It is especially the case for the flow downstream of the breach, for which the small bottom slope assumption seems to be non-coherent in regard to the rather high slopes of the dike.

Some authors proposed more complete formulations of the shallow-water equations, generally in the frame of granular flows, including the presence of a steep slope in the flow description. Among them, Savage & Hutter (1989) developed a shallow-water model for granular flows on inclined plane bed. This model was further extended to problems presenting a limited curvature of the bed (Savage & Hutter 1991), and Bouchut *et al.* (2003) developed a model appropriate for any curvature of the bottom. These two last models are useful when the bed curvature plays a significant role in the problem. These formulations are generally expressed in a local coordinate system linked to the slope and are therefore more difficult to solve in presence of complex and discontinuous topographies where the slopes themselves are difficult to define. Recently, Juez et al. (2013) proposed two 2D numerical models to solve Savage & Hutter (1989) equations: one expressed in a local coordinate system linked to the bed, and the other in a global coordinate system, to deal with complex topographies.

This paper proposes an analysis of the limitations of the small-slope assumption in the shallow water models for problems involving water flows over rather steep slopes. First, the equations including the steep slope effect are presented in one-dimensional approach and compared to the classical shallow-water equations. Models are expressed both in local and global coordinate systems. They are solved with a first-order classical finite-volume scheme, using a LHLL solver for the fluxes computation. The models are compared to each other for steady uniform flows and for fast transient flows on a fixed steep-sloped bottom. Then, a combined model able to deal with complex topographies is proposed and applied on a dike overtopping case. Finally, the impact of the models on the evaluation of bed-load sediment transport is analysed, with an application to a dike erosion by overtopping.

2 FLOW MODELLING OVER STEEP SLOPES

When modelling one-dimensional (1D) depth-averaged flow on steep slopes, two different coordinate systems (Fig. 1) can be used (Juez *et al.* 2013):

- A local coordinate system (LC), linked to the sloping bottom, with *x* and *z* the directions tangent and normal to the bed, respectively.
- A global coordinate system (GC), independent to the bed topography, with *X* and *Z* the horizontal and vertical directions, respectively.

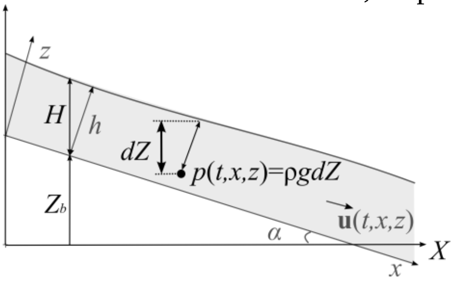

Figure 1. Definition of local and global coordinate systems for flows over a plane sloping bed.

This section presents the classical shallow-water model and a modified shallow-water model, and both models are expressed in each coordinate system.

2.1 *Classical shallow-water model (CSW)*

The classical Saint-Venant equations describe the temporal and spatial evolution of the flow depth and the depth-averaged flow velocity. These equations are based on quite restrictive assumptions:

- The fluid is incompressible.
- The streamlines are parallel to the bottom. So the component of the velocity normal to the bed is negligible. This assumption leads to a hydrostatic distribution of the pressure.
- The bottom slope α is small (cos α ≈ 1)

The Saint-Venant equations were developed in a local coordinate system (*x*,*z*), leading to the classical shallow water model (CSW – LC):

$$\begin{cases} \dfrac{\partial h}{\partial t} + \dfrac{\partial (hu)}{\partial x} = 0 \\ \dfrac{\partial (hu)}{\partial t} + \dfrac{\partial}{\partial x}\left(hu^2 + gh^2/2\right) = gh\left(S_0 - S_f\right) \end{cases} \tag{1}$$

with *t* the time, *h* the water depth perpendicular to the flow, *u* the flow velocity parallel to the bottom, and *g* the gravity. S_0 is the bottom slope:

$$S_0 = -\frac{\partial Z_b}{\partial x} = \sin\alpha \tag{2}$$

with Z_b the bed elevation in a global coordinate system. Finally, S_f is the friction term, evaluated using for instance the Manning formulation:

$$S_f = \frac{n^2 q^2}{h^{10/3}} \tag{3}$$

where $q = hu$ is the flow discharge, and *n* is the Manning coefficient.

For problems including complex topographies, the use of a local coordinate system linked to the bottom is often complicated, so, the equations are reformulated in a global coordinate system. Assuming a rather small slope, the following assumptions hold:

$$dX \cong dx,\ H \cong h,\ \mathbf{u} = (U, W) \cong (u, 0) \tag{4}$$

with *H* the vertical flow depth, and **u** the flow velocity, with components *U* and *W* in horizontal and vertical directions *X* and *Z*. With the previous assumptions, equations 1 may be reformulated in a global coordinate system (CSW – GC):

$$\begin{cases} \dfrac{\partial H}{\partial t} + \dfrac{\partial (HU)}{\partial X} = 0 \\ \dfrac{\partial (HU)}{\partial t} + \dfrac{\partial}{\partial X}\left(HU^2 + \dfrac{gH^2}{2}\right) = gH\left(-\dfrac{\partial Z_b}{\partial X} - S_f\right) \end{cases} \tag{5}$$

with

$$S_f = \frac{n^2 q^2}{H^{10/3}} \tag{6}$$

This shallow-water model expressed in a global coordinate system is the most classical depth-averaged model, and is commonly used in case of complex topography. The CSW – GC model is adequate for parallel flows over low sloping beds. It is however also generally used in case of complex topographies when the flow velocity is mostly horizontal.

2.2 *Modified shallow-water model (MSW)*

However, when the water is flowing over a steep slope, the velocity is far from being horizontal, and the small bottom slope assumption does not hold any more. Savage & Hutter (1989) developed a shallow water model for flows over constant steep slope, expressed in a local coordinate system. For this model, the fluid is assumed to be incompressible and the flow is parallel to the bottom. This last assumption leads to a hydrostatic distribution of the pressure normal to the bed (Fig. 1):

$$p(t, x, z) = \rho g (z_w - z)\cos\alpha \tag{7}$$

Accounting for the hydrostatic pressure definition (Eq. 7), the following modified shallow-water model in local coordinate is obtained (MSW – LC):

$$\begin{cases} \dfrac{\partial h}{\partial t} + \dfrac{\partial (hu)}{\partial x} = 0 \\ \dfrac{\partial (hu)}{\partial t} + \dfrac{\partial}{\partial x}\left(hu^2 + \dfrac{g\cos\alpha\, h^2}{2}\right) = gh\left(-\dfrac{\partial Z_b}{\partial x} - S_f\right) \end{cases} \tag{8}$$

where S_f can be evaluated using equation 3 for water flows, while Savage & Hutter (1989) used a Coulomb-like friction law for granular flow over a rough bed. This model reduces to the classical shallow-water model (Eq. 1) if the slope equals zero.

If the flow is mainly oriented in the longitudinal x direction, the water surface is approximately parallel to the bed. So the following relations can be used to link local and global variables (Fig. 1):

$$\begin{cases} dX = dx \cdot \cos\alpha \\ H = h/\cos\alpha \\ \mathbf{u} = (U,W) = (u\cos\alpha, -u\sin\alpha) \end{cases} \tag{9}$$

Assuming the previous relationships, the modified shallow water model (Eq. 8) can be expressed in a global coordinate system (MSW – GC):

$$\begin{cases} \dfrac{\partial H}{\partial t} + \dfrac{\partial (HU)}{\partial X} = 0 \\ \dfrac{\partial (HU)}{\partial t} + \dfrac{\partial}{\partial X}\left(HU^2 + \dfrac{g\cos^2\alpha H^2}{2} \right) \\ \qquad = gH\left(-\cos^2\alpha \dfrac{\partial Z_b}{\partial X} - \cos\alpha S_f \right) \end{cases} \tag{10}$$

with

$$S_f = \frac{n^2 q^2}{(\cos\alpha)^{10/3} H^{10/3}} \tag{11}$$

It is worth to mention that these modified shallow water models, both in LC and in GC, are appropriate only when the flow is mainly parallel to the bed. When the flow has a complex behaviour on a complex topography, the assumption on the velocity orientation is no more valid.

2.3 *Numerical resolution*

The four shallow-water models exposed previously (Eqs. 1, 5, 8 & 10) can be expressed in the following general vector form:

$$\frac{\partial \mathbf{U}}{\partial t} + \frac{\partial \mathbf{F}(\mathbf{U})}{\partial \xi} = \mathbf{S}_s + \mathbf{S}_f = \mathbf{S} \tag{12}$$

where $\mathbf{U} = (\eta, q)^T$ is the conserved variable vector, with $\eta = h$ and $q = hu$ for models in LC ($\xi = x$) and with $\eta = H$ and $q = HU$ for models in GC ($\xi = X$). The flux vector $\mathbf{F} = (q, \sigma)^T$ and the source vector $\mathbf{S}$ also vary between all models. The source vector $\mathbf{S}$ is split into a slope part $\mathbf{S}_s$ and a friction part $\mathbf{S}_f$.

These four models are solved using a first-order finite-volume scheme, with a time splitting algorithm for the friction source term:

$$\begin{cases} \mathbf{U}_i^p = \mathbf{U}_i^n + \dfrac{\Delta t}{\Delta \xi}\left(\mathbf{F}^*_{i-1/2} - \mathbf{F}^*_{i+1/2} \right) \\ \mathbf{U}_i^{n+1} = \mathbf{U}_i^p + \Delta t\, \mathbf{S}_f\left(\mathbf{U}_i^p \right) \end{cases} \tag{13}$$

where i is the cell index, n is the time index, p is the intermediate state, $\Delta\xi$ is the space step and Δt is the time step. The numerical fluxes $\mathbf{F}^*$ are computed using a first-order Harten-Lax-Van Leer (HLL) scheme (Toro 2001):

$$\mathbf{F}_1^* = q^* = \frac{\lambda_+ q_L - \lambda_- q_R + \lambda_- \lambda_+ (\eta_R - \eta_L)}{(\lambda_+ - \lambda_-)} \tag{14}$$

$$\mathbf{F}_2^* = \sigma^* = \frac{\lambda_+ \sigma_L - \lambda_- \sigma_R + \lambda_- \lambda_+ (q_R - q_L)}{(\lambda_+ - \lambda_-)} \tag{15}$$

where the subscripts L and R refer to left and right cells, respectively. The eigenvalues λ are given by:

$$\begin{cases} \lambda_\pm = u \pm \sqrt{gh} & \text{for } CSW-LC \\ \lambda_\pm = U \pm \sqrt{gH} & \text{for } CSW-GC \\ \lambda_\pm = u \pm \sqrt{g\cos\alpha h} & \text{for } MSW-LC \\ \lambda_\pm = U \pm \cos\alpha\sqrt{gH} & \text{for } MSW-GC \end{cases} \tag{16}$$

A lateralized discretisation is applied for the slope source term in the momentum equations (Fraccarollo *et al.* 2003). Due to the explicit nature of the scheme (Eq. 13), stability is dictated by the Courant condition on the time step Δt, with a coefficient CFL = 0.9 for all test cases.

For real applications, it is important to ensure the equilibrium of water at rest on a non-horizontal bed, especially for models in global coordinates. So, $(\eta_R - \eta_L)$ is replaced by $(Z_{wR} - Z_{wL})$ in equation 14 to ensure the *C*-property of the system (Bermùdez & Vasquez 1994), with $Z_w = Z_b + H$ the elevation of the water surface in global coordinates

The wetting-drying front is modelled by imposing a zero-velocity in the cells when the water depth is lower than a threshold value (typically 10^{-5} m here). This avoids to calculate unrealistically high values of the velocity $u = q/h$. Moreover, when modelling steep slopes with a global coordinate system, the slope is modelled as a succession of cells with constant slopes, leading to a step-like modelling of the slope. In this case, the flow cannot "jump" over the adjacent cell, except if the water level in the actual cell is higher than the bed level in the adjacent cell.

3 VALIDATION OF THE MODELS

Various problems include the presence of a steep slope. In this section, specific analytical test cases implying steep slopes have been selected to assess the good numerical resolution of each model. These test cases include formulations in local and global coordinate systems. The models are compared for steady uniform flows and for fast transient flows on a fixed steep-sloped bottom

3.1 *Wave on a sloping beach*

Carrier & Greenspan (1957) developed an analytical solution for wave propagation on a frictionless sloping bed. They solved analytically the classical shallow water model in global coordinate system (Eq. 5). An initial wave shape is given, with an initial zero velocity. The wave is then evolving, going up the beach and then slowly receding. As the flow does not feature velocity parallel to the bottom, the modified shallow water model is not applicable, nor the local formulations implying a water depth perpendicular to the bed. So only the CSW – GC model is used.

Figure 2 shows a comparison between the analytical and numerical profiles of the wave on steep slope ($\tan\alpha = 0.5$), for $t = 0$ - 0.18 - 0.36 s. It can be seen that the numerical and analytical profiles are really close to each other, assessing the good quality of the numerical solver. Especially, the numerical model allows reproducing precisely the wetting-drying phenomenon.

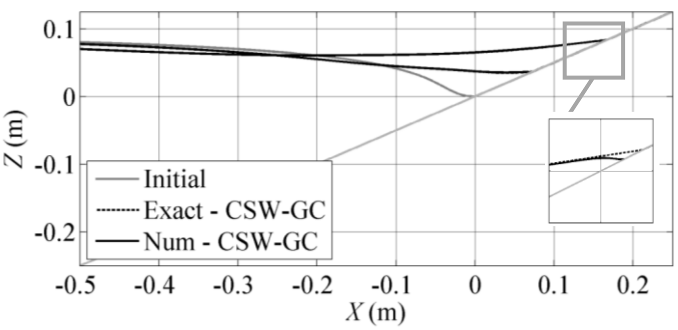

Figure 2. Wave on a sloping beach ($\tan\alpha = 0.5$): Comparison between analytical and numerical water profiles at $t = 0 – 0.18 - 0.36$ s.

3.2 *Dam break on a sloping bed*

An analytical solution of the classical 1D dam-break problem on a frictionless horizontal bed has been proposed by Stoker (1957). This solution assumes an infinite mass of fluid released at $t = 0$. For frictionless sloping beds, different analytical - or partial analytical - solutions have been proposed. Mangeney *et al.* (2000) developed an analytical solution for an infinite-volume of fluid released on a steep slope. This solution accounts for the effect of the slope on the hydrostatic pressure (Fig. 1), in a local coordinate system. This dam-break problem assumes an initial dam perpendicular to the bottom (Fig. 3), and can therefore only be used to test the numerical models in LC. In contrast, Dressler (1958) investigated the case of a finite-volume dam-break flow in a global coordinate system, assuming an initial vertical dam, but neglecting the effect of the slope in the hydrostatic pressure (Fig. 1). This test-case can be used to compare the numerical models in GC. The two initial situations are represented in figure 3.

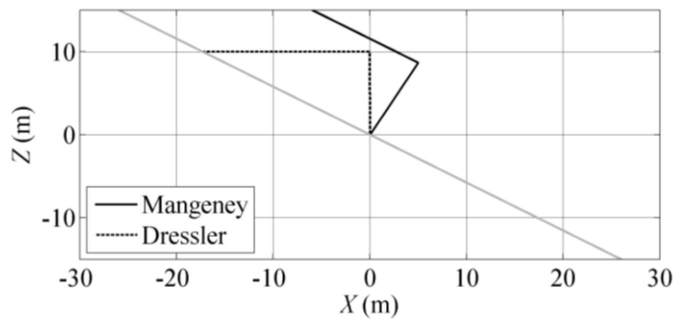

Figure 3. Initial conditions of dam-break test cases: Mangeney et al. (2000) with $h_0 = 10$ m, and Dressler (1958) with $H_0 = 10$ m

3.2.1 *Mangeney et al. (2000)*

Mangeney et al. (2000) presented the analytical solution for a dam-break granular flow on a steep sloping bed. They consider an initial infinite volume of Coulomb-frictional material, characterized by an internal friction angle δ. Here this angle is assumed to be zero, and the friction on the bottom is neglected. The initial volume has a constant water depth h_0 and zero velocity, which is obviously not a stable initial condition in case of water. They solve analytically the MSW model in local coordinates, and deduce the position of the front and back waves:

$$\begin{cases} x_{front} = \dfrac{g\sin\alpha}{2}t^2 + 2c_0 t \\ x_{back} = \dfrac{g\sin\alpha}{2}t^2 - c_0 t \end{cases} \tag{16}$$

with the initial celerity $c_0 = (gh\cos\alpha)^{0.5}$. They find the following profile between these two points:

$$h(x,t) = \frac{1}{9g\cos\alpha}\left(-\frac{x}{t} + 2c_0 + \frac{g\sin\alpha\, t}{2}\right)^2 \tag{17}$$

Imposing $c_0 = (gh)^{0.5}$ and neglecting the factor $\cos\alpha$ in equations 17, we have the equivalent analytical solution for the CSW model. And assuming a horizontal bed slope ($\sin\alpha = 0$), equation 17 reduces to Stocker profile.

Figure 4 compares the analytical and numerical results for the CSW – LC and MSW – LC models, for $h_0 = 10$ m and $\alpha = 30°$. It can be observed that the front and the back waves propagate faster with the classical shallow water model, both analytically and numerically. The front wave position is globally well estimated by the numerical models, while the errors are more important for the back wave. The numerical models seem to overestimate the propagation of the back wave. However, looking at the depth profile (Fig. 4b), it can be seen that the numerical solution is really close to the analytical results, except near x_{front} and x_{back}. It can also be observed that the difference between CSW and MSW model is not really important.

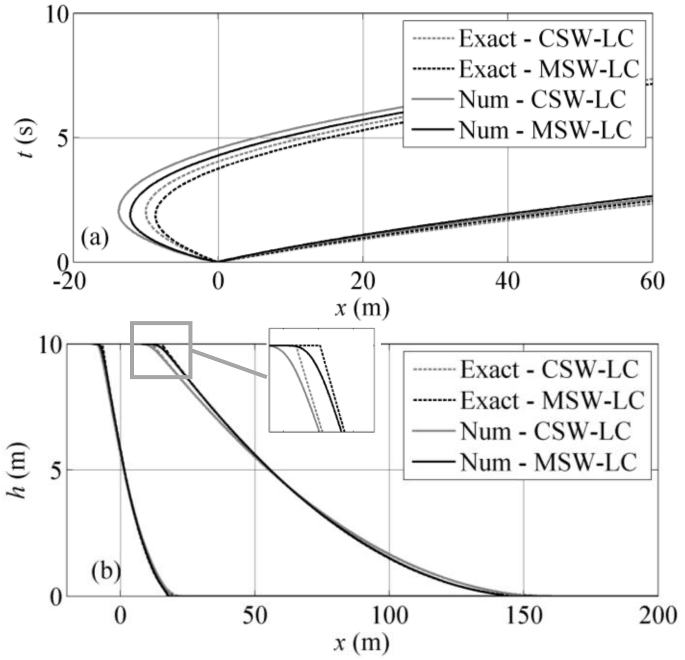

Figure 4. Mangeney et al. (2000) dam-break: comparison between analytical (--) and numerical (-) solutions ($h_0 = 10$ m, $\alpha = 30°$) for CSW – LC and MSW – LC models: (a) front wave and back wave in *x-t* plane – (b) profile of the water depth *h* for $t = 1$ and 5 s.

3.2.2 *Dressler (1958)*

In contrast with the previous dam-break solution, Dressler (1958) focused on the CSW – GC model for an initial finite volume of water at rest ($u_0 = 0$, $Z_{w0} = C^{st}$) behind a vertical dam (Fig. 3), on a gentle-sloping bed. He developed an analytical formulation for the front and back wave positions. As the reservoir volume is finite, the back wave travels upward until reaching the upstream point of the reservoir at $t = t_B$. Then a moving downstream boundary travels downward, corresponding to the emptying of the reservoir ($H = 0$):

$$\begin{cases} X_{front} = \dfrac{g\tan\alpha}{2}t^2 + 2c_0 t \\ X_{back} = \dfrac{g\tan\alpha}{4}t^2 - c_0 t \quad for \quad t \le t_B = \dfrac{2c_0}{g\tan\alpha} \\ X_{back} = \dfrac{g\tan\alpha}{2}t^2 - 2c_0 t + \dfrac{H_0}{\tan\alpha} \quad for \quad t \ge t_B \end{cases} \qquad (20)$$

with $c_0 = (gH_0)^{0.5}$. The same development has been applied to find the same back- and front-waves positions for the MSW – GC model. An equivalent formulation is obtained for the same initial conditions, by replacing the gravity g in equation 20 by ($g\cos^2\alpha$) and with $c_0 = (g\cos^2\alpha H_0)^{0.5}$.

Figure 5a shows the comparison between analytical and numerical propagation of the front and back waves for $H_0 = 10$ m and $\alpha = 30°$, while figure 5b compares the numerical water profiles after 1 and 2 s. As for Mangeney dam-break, the propagation of the front wave is correctly modelled numerically, while the back wave propagation is less precise before the reservoir emptying (Fig. 5a). But globally numerical results are really close to analytical solutions. As for dam-break in LC, the numerical water profiles with CSW and MSW models give comparable results, except at the wave head and toe (Fig. 5b).

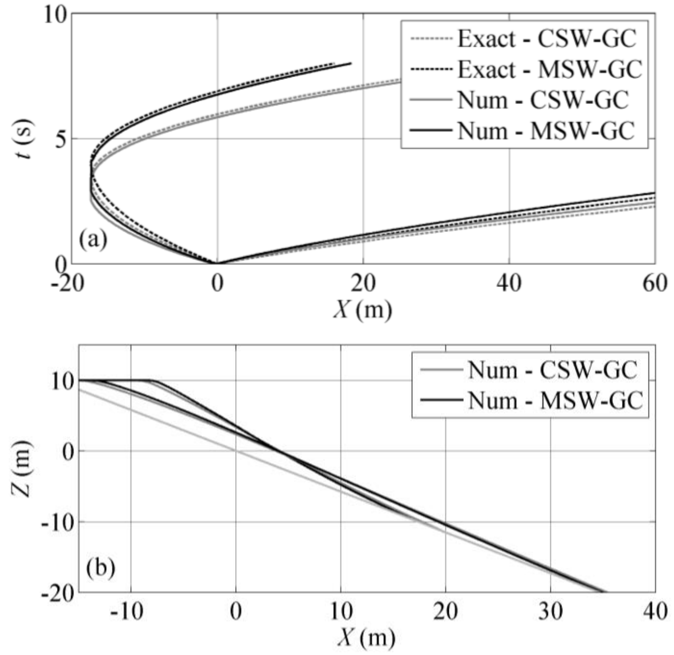

Figure 5 Dressler. (1958) dam-break: comparison between analytical (--) and numerical (-) solutions ($H_0 = 10$ m, $\alpha = 30°$) for CSW – GC and MSW – GC models: (a) front wave and back wave in *x-t* plane – (b) profile of the water for $t = 1$ and 2 s.

It can be globally concluded from the dam-break test cases that the numerical resolution of the four models give accurate results, and that the MSW and CSW models give comparable results for fast transient flows.

3.3 *Steady uniform flow on a sloping bed*

The previous test cases analyzed the ability of the four numerical models to simulate fast transient flows. We showed that, for such transient cases, the more precise MSW model does not improve significantly the results. So, this section aims at showing the impact of the MSW model on a steady uniform flow, still on a steep slope.

For steep slope problems, the uniform flow is supercritical, so we impose a given inflow q_0 and uniform water depth h_u as upstream boundary condition, while the downstream boundary is a free outflow. To simulate a steady uniform flow, the modification suggested by Bermùdez & Vasquez (1994) (the replacement of ($\eta_R - \eta_L$) by ($Z_{wR} - Z_{wL}$) in equation 14) is not any more valid and moreover not required as the aim is not to model the equilibrium of the water at rest. So, equation 14 is used without any modification for this test-case.

Figure 6 compares water profiles in steady uniform flows for the four models, with $q_0 = 0.05$ m³/s/m, and h_u given by:

$$h_u = \left(\frac{n^2 {q_0}^2}{\sin\alpha} \right)^{3/10} \tag{21}$$

with $n = 0.017\ \mathrm{s\,m^{-1/3}}$. For models in GC, the upstream depth condition is $H_u = h_u/\cos\alpha$.

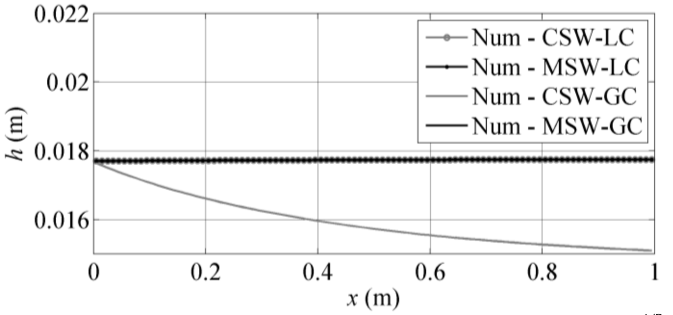

Figure 6. Steady uniform flow – $\alpha = 30°$, $n = 0.017\ \mathrm{s\,m^{-1/3}}$, $q_0 = 0.05\ \mathrm{m^3/s/m}$, with h_u given in equation 21.

It can be observed on figure 7 that the steady uniform flow is obtained for the given upstream condition, except with CSW – GC model. Indeed, for this model, the uniform water depth given in equation 21 is not valid. The equilibrium uniform water depth for equation 5 is:

$$-\frac{\partial Z_b}{\partial X} = \tan\alpha \Leftrightarrow S_f \cong \frac{n^2 q^2}{H^{10/3}} \quad \Rightarrow H_u = \left(\frac{n^2 q^2}{\tan\alpha} \right)^{3/10} \tag{22}$$

This difference in the uniform water depth for the classical SW model in GC is mainly due to the assumption of a horizontal velocity, and to the consecutive change of variables (Eq. 4) from LC to GC. The comparison between the classical uniform depth h_u (Eq. 21), its vertical projection $h_u/\cos\alpha$, and the uniform depth H_u of the CSW – GC model (Eq. 22) is exposed in figure 7. It can be seen that the difference between the real uniform depth and the approximation of the CSW – GC model starts to be important for slope angles higher than 15°, while the vertical projection of h_u is already higher for slope angles of 10°.

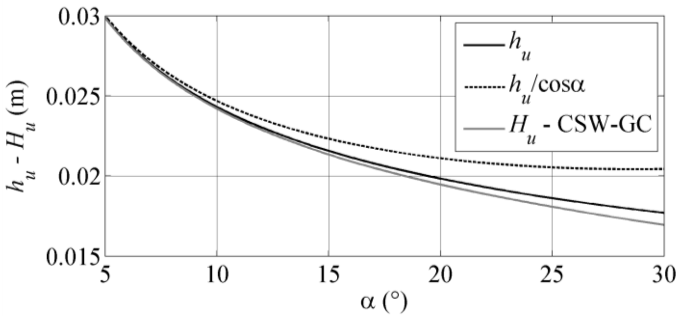

Figure 7. Uniform water depth (Eq. 21) and approximate uniform depth of the CSW – GC model (Eq. 22) as a function of the bed slope angle.

So it can be concluded that the commonly used CSW – GC model gives an acceptable description of the flow in fast transient conditions, but this model can generate important errors when used for steady flows.

4 APPLICATION TO A DIKE OVERTOPPING TEST-CASE

Let us now analyse the particular case of an idealized flow overtopping a dike, as sketched in figure 8. In this particular case, we have a rather quiet flow upstream of the dike, where we can assume a horizontal velocity. On the downstream slope however, water is gravitationally flowing downslope, with a velocity mainly oriented parallel to the downstream dike slope (Fig. 8).

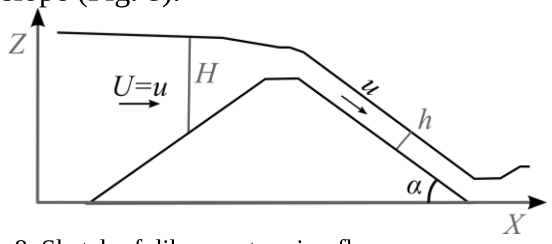

Figure 8. Sketch of dike overtopping flow

As the topography is rather complex, with a non-constant slope angle, it is preferable to use a model in a global coordinate system to represent the flow over the dike. This kind of problems, especially when modelling the erosion of the dike, is generally solved using the CSW – GC model. We propose here to compare these results with a new combined model, using the MSW – GC model to represent the flow over the downstream dike slope.

4.1 *New combined shallow-water model*

The new combined shallow water model (NewSW – GC) is a simple combination of the MSW – GC model for gravitational parallel flows over rather steep slopes, with the CSW – GC model for other flows, which are assumed to be mostly horizontal. The transition between both models is given by:

$$\begin{aligned} &if \left(\frac{\Delta H}{\Delta X} < 0.1\ \&\ \alpha > 0 \right) \quad \Rightarrow MSW-GC \\ &else \quad \Rightarrow CSW-GC \end{aligned} \tag{23}$$

4.2 *Steady flow over a dike*

Figure 9 compares the results obtained with the CSW – GC model and with the NewSW – GC model for a steady flow over a 0.2 m high dike, with upstream and downstream slopes of $\tan\alpha = 0.5$, and a 10 cm long crest, with a constant discharge of $0.025\ \mathrm{m^3/s/m}$.

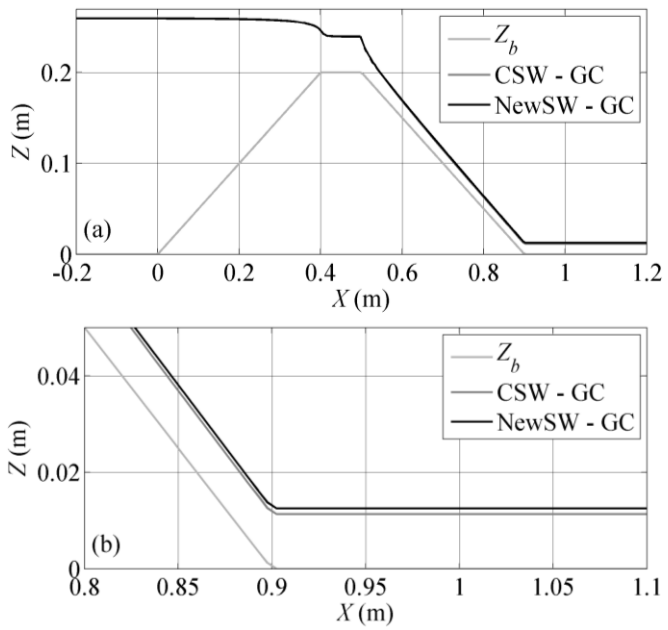

Figure 9. Steady flow over a fixed dike: $H_d = 0.2$ m, $S_{0u} = S_{0d} = 0.5$, $q_0 = 25$ l/s/m

The new combined model gives results really close to the classical model for the dike overtopping test case (Fig. 9). These flow conditions are indeed far from uniform flow conditions, and so the differences between the MSW – GC model and the CSW – GC model on the downstream dike slope are quite low. So for pure hydrodynamic flow over a dike, the CSW – GC model can be used without generating important errors.

5 INFLUENCE ON SEDIMENT TRANSPORT

To fully model an earthen dike overtopping problem, it is also important to analyse the impact of the use of a simplified model as the CSW – GC model on the sediment transport evaluation.

5.1 *Sediment transport formulation*

This analysis will focus on bed-load sediment transport. Suspended sediments are indeed transported by the flow velocity, and will therefore behave as hydrodynamic flows. Bed-load however depends on the shear stress on the bed:

$$\tau_b = \rho g h S_f \quad \Rightarrow \tau_* = \frac{n^2 q^2}{(s-1) d h^{7/3}} \tag{24}$$

with τ_b the bed shear stress and its non-dimensional value $\tau_* = \tau_b/(\rho(s\text{-}1)gd)$ (Shields parameter), ρ the water density, and $s = \rho_s/\rho$ the ratio of sediment and water densities. Various empirical relations have been developed to evaluate the bed-load transport. One of the most common equations has been elaborated by Meyer-Peter & Müller (1948):

$$q_s = 8\sqrt{g(s-1)d^3}\left(\tau_* - \tau_{*cr}\right)^{1.5} \tag{25}$$

with q_s the sediment discharge (m³/s/m), d the grain diameter, and $\tau_{*cr} = 0.047$ the threshold Shields parameter for sediment motion. Equation 25 shows that bed-load transport is linked to the flow conditions only through the shear stress. This shear stress, depending on the water depth h and on the flow q (Eq. 24), is assumed to be tangent to the bed. But when using the CSW – GC model, the shear stress is evaluated using the vertical water depth H, and the bed shear stress is assumed to be mostly horizontal, which is questionable on steep slopes.

Figure 10 compares the evaluated bed-load transport for uniform flows as a function of the bed slope angle, in which the Shields parameter is evaluated in three different ways:

- The classical Shields parameter $\tau_*(h_u)$ (Eq. 24), with h_u given by equation 21
- The Shields parameter evaluated with the vertical projection of h_u: $\tau_*(h_u/\cos\alpha)$
- The Shields parameter evaluated using the uniform water depth of the CSW – GC model: $\tau_*(H_u)$, with H_u given by equation 22.

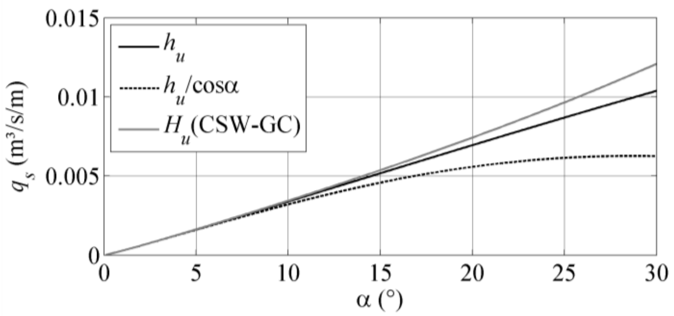

Figure 10. Sediment transport evaluation in comparison with the slope angle ($q = 0.05$ m³/s/m, $d = 6.1$ mm, $n = 0.0138$)

It can be seen on figure 10 that the assumption of $h_u \sim= H_u$ can be used to evaluate the bed-load sediment transport for slope angles lower than 10°. For slopes higher than 10°, it is important to evaluate the Shields parameter with the appropriate perpendicular water depth h. The approximate uniform depth of the CSW – GC model leads to an overestimation of the sediment transport for slope angles higher than 15°.

5.2 *Shallow-water – Exner models*

To model a flow-erosion process, the shallow water equations for mass and momentum conservation can be coupled with the Exner equation for sediment conservation in global coordinates (Cunge & Perdreau 1973):

$$\frac{\partial Z_b}{\partial t} + \frac{1}{1-\varepsilon_0}\frac{\partial q_s}{\partial X} = 0 \tag{26}$$

with ε_0 the bed porosity and q_s the sediment transport, evaluated using equation 25. This Exner equation is coupled to the CSW - GC model (Eq. 5), with $\tau_*(H)$, to form the classical shallow-water – Exner model in GC (CSWE – GC). This model (Eqs.

5 & 26) is solved in a coupled way using the same first order finite volume scheme, with a lateralised HLL solver for the fluxes (Goutière et al. 2008).

The Exner equation can also be coupled with the MSW – GC model, with $\tau_*(h = H\cos\alpha)$, forming the MSWE – GC model. This model is numerically solved in the same way as the CSWE – GC model. Finally, both models can be combined to form the NewSWE – GC model, using the criterion given in equation 23.

5.3 *Application on dike overtopping test case*

The CSWE – GC and the NewSWE – GC models are applied on the experimental dike overtopping test case reported in (Van Emelen *et al.* 2013). A 0.20 m high sand dike is placed in a 10 m long and 0.2 m wide horizontal flume. The dike crest length is 0.10 m, and the upstream and downstream slopes are 1V:2H, with a 5 cm thick sand layer downstream of the dike. The sand characteristics are: $s = 2.65$, $d_{50} = 0.61$ mm, $\varepsilon_0 = 0.43$, $n = 0.0138$ s m$^{-1/3}$. The initial water level is 0.17 m upstream of the dike, and the inflow is 5 l/s. The initial time (t = 0 s) corresponds to the beginning of overtopping, and the mesh size is $\Delta x = 0.02$ m.

Figure 11 compares the experimental water and dike profiles after 24 s of overtopping with the numerical profiles obtained with the CSWE – GC and NewSWE – GC models.

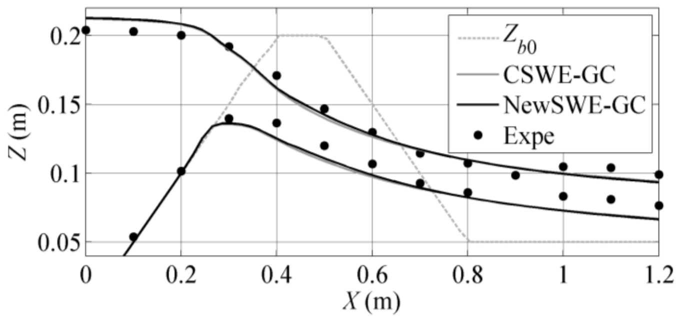

Figure 11. Dike overtopping: dike and water profiles at t = 24 s with the classical SWE model and the new combined model.

The difference between the two numerical dike profiles is rather small, and they globally simulate well the dike profile (Fig. 11). The NewSWE – GC model is eroding a little less on the downstream dike slope, but this small difference has no impact on the crest elevation, and therefore both models generate a comparable overflow hydrograph.

6 CONCLUSIONS

The present paper analyses the limitations of the shallow water assumptions to simulate flows over steep slopes. The classical shallow water model is compared to a modified shallow water model accounting for the impact of the steep slope on the flow.

For rapid transient flows, such as dam-break flows or dike overtopping, it is shown that nearly no difference appear between classical and modified models. So the commonly used classical shallow water model gives an acceptable description of the flow in fast transient conditions. For steady uniform flows however, differences are visible for bed angles higher than 10°, indicating that classical shallow flows are not suitable for uniform flows on steep slopes.

The impact of the classical shallow water assumptions on the sediment transport evaluation has also been evaluated, and the same conclusions hold true for sediment transport: the classical shallow water model is suitable for fast transient flows, but more accurate models should be used when modelling erosion for steady uniform flows.

REFERENCES

Bermùdez, A., Vázquez, M.E. 1994. Upwind methods for hyperbolic conservation laws with source terms. *Computers and Fluids*, 23(8), 1049-1071.

Bouchut, F., Mangeney-Castelnau, A., Perthame, B., & Vilotte, J. P. 2003. A new model of Saint Venant and Savage-Hutter type for gravity driven shallow flows, *C. R. Acad. Sci. Paris sér.* I, 336, 531– 536.

Carrier, G. F., & Greenspan, H. P. 1958. Water waves of finite amplitude on a sloping beach, *J. Fluid Mech*., 4, 97– 109.

Cunge, J. A., & Perdreau, N. 1973. Mobile bed fluvial mathematical models. *Houille Blanche*, 28(7), 561–580.

Dressler, R. H. 1958. Unsteady non-linear waves in sloping channels, *Proc. R. Soc. London Ser*. A, 247, 186–198.

Fraccarollo, L., Capart, H., Zech, Y. 2003. A Godunov method for the computation of erosional shallow water transients. *Internat. J. Numer. Method. Fluid*. 41, 951- 976.

Goutière, L., Soares-Frazão, S., Savary, C., Laraichi, T., Zech, Y. 2008. One-dimensional model for transient flows involving bedload sediment transport and changes in flow regimes. *J. Hydraul. Eng.*, 134(6), 726–735.

Juez, C. Murillo, J., & García-Navarro, P. 2013. 2D simulation of granular flow over irregular steep slopes using global and local coordinates. *J. Comput. Phys.* 255, 166–204.

Mangeney, A., Heinrich, P., and Roche, R. 2000. Analytical solution for testing debris avalanche numerical models. *Pure Appl. Geophys.* 157, 1081-1096.

Meyer-Peter, E., and Müller, R. 1948. Formulas for bed load transport. *Proc. 2nd IAHR Congress*, Stockholm, Sweden, 39-64.

Savage, S. B. & Hutter, K. 1989 The motion of a finite mass of granular material down a rough incline. *J. Fluid Mech.* 199, 177–215.

Savage, S. B. & Hutter, K. 1991. The dynamics of avalanches of granular materials from initiation to runout. Part I. Analysis. *Acta Mech*. 86, 201–223.

Stoker, J. J. 1957. *Water Waves*, Interscience Publishers, New York.

Toro, E. 2001. *Shock-Capturing Methods for Free-Surface Shallow Flows*, Wiley, New-York.

Van Emelen, S., Ferbus, V., Spitaels, T., Zech, Y., and Soares-Frazão, S. 2013. Experimental investigation of the erosion of a sand dike by overtopping. *Proc. 35th IAHR World Congress*, Chengdu, China.